Methods and Applications

Cost-Effectiveness Analysis of Vaccination Compliance Strategies Using a Novel Hybrid Model for Influenza Vaccination

Dongfang You[1,2]; Yi Zhou[1]; Yan Yan[3]; Feng Chen[1,4]; Mengyi Lu[2,4,#]; Fang Shao[1,#]

ABSTRACT

Introduction: The cost-effectiveness of vaccination strategies plays a crucial role in managing infectious diseases such as influenza within public health systems. This study evaluated the cost-effectiveness of vaccination compliance strategies by comparing an "adherence" strategy, which promoted continuous vaccination uptake, with a "volunteer" strategy through model-based simulations.

Methods: We developed a novel hybrid model that integrates continuous-time agent-based models (ABMs) with a Markov model to simulate vaccination behaviors and disease dynamics at the individual level. The model incorporated socioeconomic factors, vaccine efficacy, and population interactions to evaluate the long-term health outcomes and associated costs of different vaccination compliance strategies.

Results: Simulation results demonstrated that the "adherence" strategy significantly enhanced vaccination coverage and reduced influenza cases, yielding an incremental cost-effectiveness ratio (ICER) of 33,847 CNY per quality-adjusted life year (QALY) gained, indicating superior cost-effectiveness compared to the "volunteer" strategy.

Discussion: Our findings support implementing targeted influenza vaccination compliance strategies, presenting an innovative approach to strengthening public health interventions and enhancing vaccination program effectiveness. The hybrid model shows promise in informing public health policy and practice, warranting further investigation of its applications across diverse public health contexts.

Influenza vaccination represents a cornerstone of public health interventions for controlling this highly transmissible disease. However, in countries like China, where vaccination remains voluntary and lacks public funding, achieving adequate vaccination coverage presents significant challenges (*1–2*). The "volunteer" strategy, which depends on individuals' self-funded participation, has consistently resulted in suboptimal coverage rates and elevated outbreak risks. This situation necessitates innovative approaches to enhance vaccination compliance. The "adherence" strategy, designed to encourage previously vaccinated individuals to maintain their vaccination status through consistent advocacy, healthcare provider interventions, and financial incentives, offers a more pragmatic alternative to mandatory vaccination policies.

While existing vaccination strategies and their corresponding models have proven effective in cost-effectiveness analyses (CEAs), they often fail to capture the complex interplay between individual behaviors, social dynamics, and economic factors (*1–3*). Traditional Markov models, though effective for disease progression simulation, cannot adequately represent individual-level dynamics and social interactions that significantly influence vaccination decisions. Similarly, compartmental models, such as the SEIR model, while valuable for understanding disease transmission dynamics, tend to oversimplify population heterogeneity and the nuanced aspects of vaccination behavior (*4–6*).

To address these methodological limitations, we propose an innovative hybrid modeling approach that integrates continuous-time agent-based models (ABMs) with Markov models. The continuous-time ABM component enables detailed simulation of disease transmission and individual interactions within populations, providing granular insights into the temporal evolution of vaccination compliance strategies (*5*). By combining this with a Markov model that captures the stochastic nature of vaccination decisions across multiple cycles, we can comprehensively analyze the long-term cost-effectiveness of different vaccination strategies. Our hybrid model provides a sophisticated framework for evaluating sustained vaccination compliance strategies, offering more precise and nuanced assessments of the

benefits and costs associated with various vaccination approaches.

In summary, this study presents a sophisticated analytical tool that leverages the complementary strengths of continuous-time ABMs and Markov models to conduct comprehensive, long-term CEA of vaccination compliance strategies. This hybrid model demonstrates significant potential for informing evidence-based public health policy and practice.

METHODS

We propose a novel hybrid modeling framework that integrates a continuous-time agent-based susceptible-exposed-infected-hospitalized-removed/recovered (SEIHR) model with a Markov model for the cost-effectiveness analysis of influenza vaccination compliance strategies (*4*–*5*). Schematic representations of the agent-based SEIHR and hybrid models are provided in Figures 1A and 1B, with a comprehensive description included in the Methods section of the Supplementary Material (available at https://weekly.chinacdc.cn/).

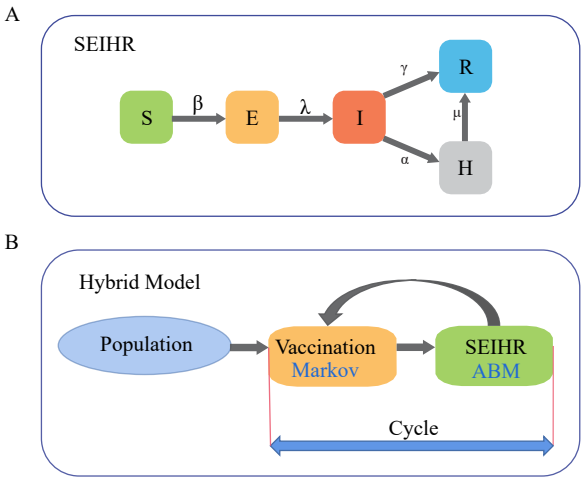

FIGURE 1. Framework of the SEIHR model and the proposed hybrid model for influenza vaccination compliance strategy analysis. (A) SEIHR model. (B) The proposed hybrid model.
Note: SEIHR model with compartments or states: susceptible (S), exposed (E), infectious (I), hospitalized (H), and removed/recovered (R). For every cycle, the individual vaccination uptake is modeled through a Markov model, contingent upon infection status and prior vaccination history, followed by an ABM simulation to depict influenza spread dynamics. This iterative process repeats for each cycle.
Abbreviation: SEIHR=susceptible-exposed-infected-hospitalized-removed/recovered; ABM=agent-based model.

The SEIHR model, adapted from traditional compartmental models, simulates influenza transmission within a randomly mixed population by incorporating individual-level interactions and disease dynamics. This model has been transformed into an agent-based format, with its deterministic nature validated against stochastic ABMs through previous studies (*5*–*6*).

Our proposed hybrid model iteratively transitions between the ABM simulation of one cycle and a Markov model-based vaccination process for the subsequent cycle, continuing this sequence for a predefined number of cycles to evaluate long-term vaccination compliance strategies.

We conducted simulations to demonstrate the application of our hybrid model in long-term CEA of influenza vaccination compliance strategies. Table 1 presents the parameter configurations used in the simulation. The baseline population was stratified according to age group proportions (≤18, 20–64, and ≥65 years old) derived from the China Statistical Yearbook 2023, with the national gross domestic product (GDP) per capita set at 85,698 Chinese Yuan (CNY) (*7*). The population size N was established at 1,000,000. Daily utility values for each state were derived from QALYs in the literature divided by 365 (*8*–*9*). Daily costs for infected (I) and hospitalized (H) states were derived by dividing the total outpatient and inpatient costs from the literature by their respective average duration of care (*3*,*10*). For the middle age group (20–64 years), the daily hospitalization cost incorporated lost labor productivity based on GDP per capita divided by 365. Vaccine cost was fixed at 67.1 CNY per dose (*1*). Each cycle represented one year (365 days), with a 5% discount rate applied to both costs and utilities (QALYs) over 5 cycles (5 years) (*11*).

Two distinct vaccination compliance strategies were evaluated. The "volunteer" strategy served as a baseline approach, where each agent's vaccination probability per cycle was calculated by multiplying the age group-specific baseline coverage (c) by previous infection multiplier (m_{ci}) and vaccination multiplier (m_{cv}) when applicable (i.e., $cm_{ci}m_{cv}$ for previously vaccinated individuals, and cm_{ci} for those not previously vaccinated) (*12*–*15*). The "adherence" strategy differed fundamentally by implementing scheduled follow-up vaccinations in subsequent cycles for individuals who received vaccination within a particular cycle. Given the stochastic nature of the ABM, we performed 1,000 simulation replicates and conducted probabilistic sensitivity analysis (PSA) to evaluate the economic

TABLE 1. Overview of vaccination compliance strategies and their parameters.

Parameters	Age groups			References
	Age group 1 (≤19)	Age group 2 (20–64)	Age group 3 (≥65)	
Baseline proportion	0.2137	0.6375	0.1488	(*7*)
Baseline vaccination coverage, c	0.251	0.067	0.267	(*12*)
Previous vaccination multiplier for coverage, m_{cv}	1.5	1.5	1.5	–
Previous infection multiplier for coverage, m_{ci}	NI: 0.8 I: 1 IH: 2	NI: 0.8 I: 1 IH: 2	NI: 0.8 I: 1 IH: 2	–
Discount rate	0.05	0.05	0.05	(*11*)
Rate from S to E, β	0.225	0.107	0.088	(*3*)
Rate from E to I, λ	0.5	0.5	0.5	(*3*)
Rate from I to H, α	0.0141	0.0193	0.0421	(*13*)
Rate from H to R, μ	0.0847	0.0847	0.0847	(*2*)
Rate from I to R, γ	0.1613	0.1613	0.1613	(*2*)
Vaccination multiplier for the rate from S to E, $m_{\beta v}$	0.36	0.41	0.42	(*14–15*)
Vaccination multiplier for the rate from I to H, $m_{\alpha v}$	0.47	0.68	0.68	(*3*)
Cost per day (CNY)	I : 157 H: 833	I: 157 H: 1068	I: 157 H: 833	(*7*,*10*)
QALY	S: 0.8434 E: 0.8434 I : 0.6216 H: 0.6132 R: 0.8434	S: 0.8434 E: 0.8434 I : 0.5939 H: 0.4913 R: 0.8434	S: 0.8071 E: 0.8071 I : 0.5733 H: 0.4128 R: 0.8071	(*8–9*)
Vaccination cost per dose (CNY)	67.1	67.1	67.1	(*1*)
Attack rate	0.01	0.01	0.01	–

Note: S, E, I, H, and R represent the states of the SEIHR model. For the previous infection multiplier for coverage, NI, I, and IH represent no infection, infection without hospitalization, and infection with hospitalization, respectively. A dash ("-") indicates that the values are self-determined in the absence of relevant references.
Abbreviation: CNY=Chinese Yuan; SEIHR=susceptible-exposed-infected-hospitalized-removed/recovered; QALY=quality-adjusted life year.

outcomes of these strategies. The analysis included the incremental cost-effectiveness ratio (ICER), cost-effectiveness plane (CEP), cost-effectiveness acceptability curves (CEACs), cost-effectiveness acceptability frontier (CEAF), and expected value of perfect information (EVPI). The PSA incorporated random variable probability distributions for attack rate, baseline vaccination coverage, QALY multiplier, and cost per day multiplier, with detailed parameter settings available in Supplementary Table S1(available at https://weekly.chinacdc.cn/).

All analyses were performed using R (version 4.2.0; R Core Team, Vienna, Austria) with the 'ABM', 'rcea', 'hesim', and 'ggplot2' packages. The simulation R code is accessible in the Supplementary Material.

RESULTS

The simulation results from our proposed hybrid model are summarized in Table 2 and Figure 2, with comprehensive details provided in Supplementary Table S1 and Supplementary Figure S1 (available at https://weekly.chinacdc.cn/).

Comparative analysis of the "adherence" and "volunteer" vaccination compliance strategies revealed an incremental vaccination ratio of 133.800%, indicating a substantial increase in vaccination coverage. The detailed vaccination coverage rates across cycles are presented in Supplementary Table S1 and Supplementary Figure S1. The strategy achieved significant reductions in healthcare utilization, with decremental ratios of 16.276%, 15.859%, and 19.746% for total infections, inpatient cases, and outpatient cases, respectively. These reductions demonstrate the potential public health benefits associated with enhanced vaccination coverage.

The economic analysis revealed an incremental cost of 3,067 CNY and an incremental quality-adjusted life year (QALY) gain of 0.091 per 1,000 individuals over the five-year horizon. With a willingness-to-pay (WTP) threshold set at 85,698 CNY (equivalent to the national GDP per capita), the net monetary benefit

TABLE 2. Summary of the hybrid model simulation results for influenza vaccination strategies.

Outcome	"Adherence" *vs.* "Volunteer" [Estimate (95% *CI*)]
Incremental vaccination number	824.075 (823.988, 824.162)
Decremental infection number	22.589 (22.519, 22.658)
Decremental inpatient number	19.656 (19.593, 19.719)
Decremental outpatient number	2.933 (2.922, 2.944)
Incremental vaccination ratio (%)	133.800 (133.784, 133.816)
Decremental infection ratio (%)	16.276 (16.231, 16.320)
Decremental inpatient ratio (%)	15.859 (15.814, 15.905)
Decremental outpatient ratio (%)	19.746 (19.679, 19.813)
WTP threshold (CNY)	85,698
Incremental QALYs	0.091 (0.079, 0.102)
Incremental costs (CNY)	3,067 (−3,047, 8,772)
Incremental NMB (CNY)	4,699 (−1,939, 11,606)
ICER (CNY per QALY)	33,847

Note: The outcome values are for every 1,000 individuals for 5 years.
Abbreviation: *CI*=confidence interval; CNY=Chinese Yuan; ICER=incremental cost-effectiveness ratio; NMB=net monetary benefit; QALY=quality-adjusted life year; WTP=willingness to pay.

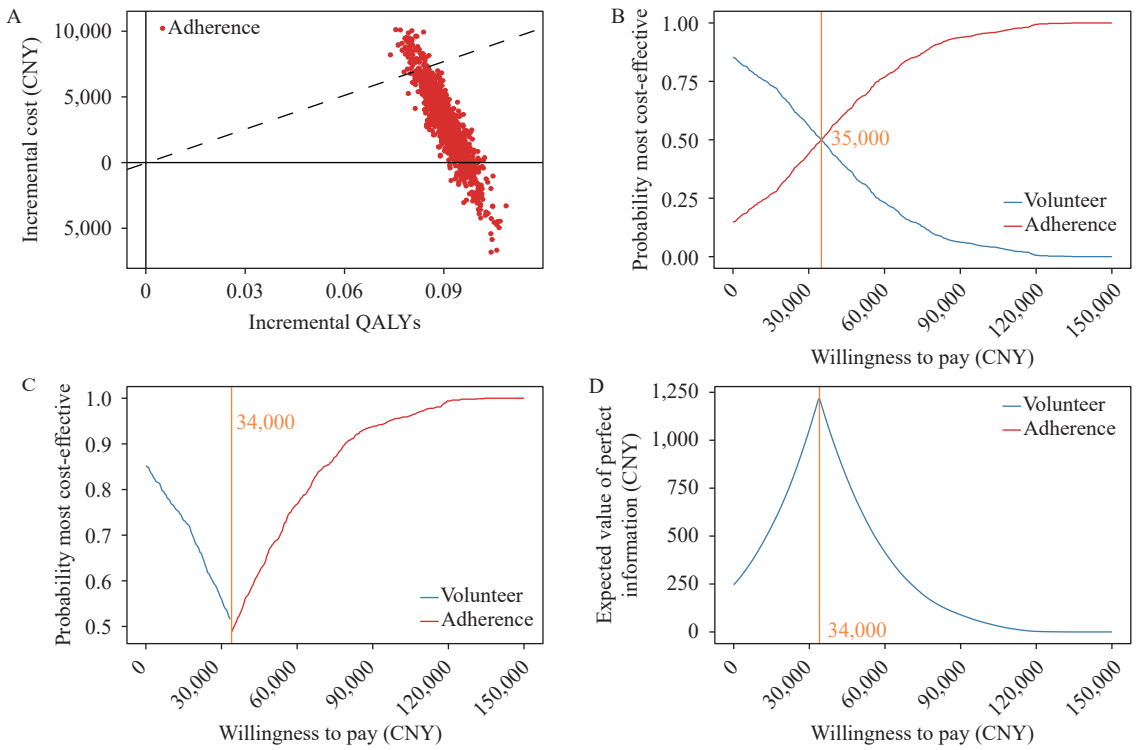

FIGURE 2. Cost-effectiveness analysis results for the hybrid model simulations. (A) The cost-effectiveness plane; (B) The cost-effectiveness acceptability curves; (C) The cost-effectiveness acceptability frontier; (D) The expected value of perfect information.
Note: In panel A, the dashed line represents the WTP threshold (85,698 CNY). The costs and QALYs are reported for every 1,000 individuals for 5 years. The population size is *N*=100,000 with 1,000 simulation replicates.
Abbreviation: CNY=Chinese Yuan; QALY=quality-adjusted life year; WTP=willingness to pay.

(NMB) was estimated at 4,699 CNY, yielding an incremental cost-effectiveness ratio (ICER) of 33,847 CNY per QALY gained.

Comparative analysis of the long-term effects demonstrated that the "adherence" strategy exhibited superior cost-effectiveness compared to the "volunteer"

strategy. This superiority was evidenced through multiple analytical tools, including the cost-effectiveness plane (CEP), cost-effectiveness acceptability curves (CEACs), cost-effectiveness acceptability frontier (CEAF), and expected value of perfect information (EVPI), across various WTP thresholds with discrete increments of 500 CNY. The results are presented in Figure 2.

The CEP (Figure 2A) illustrates the relationship between incremental QALYs (x-axis) and incremental costs (y-axis), with each point representing a distinct simulation iteration. The WTP threshold (85,698 CNY) is depicted by a dashed line, below which points are considered cost-effective. Analysis revealed that only 7.1% of points were cost-ineffective, while 14.8% demonstrated dominance (both cost-saving and health-improving).

The CEAC (Figure 2B) and CEAF (Figure 2C) demonstrate the probability of each strategy achieving optimal cost-effectiveness across different WTP thresholds. The analysis indicates that the "adherence" strategy demonstrates a higher probability of cost-effectiveness at WTP values exceeding the ICER (33,847 CNY), suggesting its preferential status compared to the "volunteer" strategy.

The EVPI analysis (Figure 2D) quantifies the potential value of acquiring additional information to reduce decision uncertainty. The analysis reveals peak EVPI values near the ICER threshold, indicating that decision-makers might find value in investing in additional research to clarify the cost-effectiveness of these vaccination strategies at this critical threshold point.

The findings of the PSA aligned with the primary analyses. Detailed results are presented in the Supplementary Tables S3–S4, Supplementary Figures S2–S3 (available at https://weekly.chinacdc.cn/).

DISCUSSION

This study introduces an innovative hybrid modeling framework that integrates a continuous-time agent-based SEIHR model with a Markov model to conduct comprehensive cost-effectiveness analyses of influenza vaccination compliance strategies. Our approach leverages the granularity of continuous-time ABMs for simulating influenza dynamics, offering enhanced precision for modeling individual interactions and disease transmission compared to discrete-time alternatives. The integration with the Markov model enables robust assessment of vaccination compliance across multiple cycles, providing a framework for evaluating long-term strategic outcomes. By more accurately reflecting real-world epidemiological contexts of influenza transmission, this hybrid model overcomes key limitations of traditional models that typically focus on short-term, single-cycle analyses of infectious disease dynamics (*1*,*2*,*5*,*6*). The versatility of our proposed framework makes it particularly valuable for evaluating a broad spectrum of infectious disease interventions.

Our findings demonstrate that the "adherence" strategy represents a cost-effective alternative to the "volunteer" strategy for influenza vaccination when considering the willingness-to-pay threshold of 85,698 CNY. These results underscore the importance of implementing vaccination compliance strategies that not only enhance vaccination coverage but also mitigate the health burden of influenza in a cost-effective manner.

Despite the robust nature of our hybrid model, several limitations warrant consideration. The assumption of random interactions among agents in the ABM does not fully capture the complexities of real-world contact patterns, including social networks and behavioral determinants. Additionally, the model simplifies certain aspects of influenza transmission dynamics by excluding protective measures, population mobility patterns, and mortality outcomes. The vaccination compliance strategies modeled also represent idealized scenarios, which may limit the generalizability of our findings.

Furthermore, while our model provides innovative insights into vaccination strategies, it has not yet been validated against real-world epidemiological data. As such, our hybrid model should be viewed as a framework to inform public health policy and practice rather than as a direct policy prescription tool. Future research directions include refining the model by incorporating more realistic contact patterns, validating against empirical data, and exploring applications to specific target populations, such as elderly individuals, healthcare workers, and those with comorbidities. The adaptability of our hybrid model framework suggests potential applications beyond influenza vaccination to a broader range of public health interventions. Future investigations could explore the integration of discrete-time agent-based models and decision trees, further enhancing the model's flexibility and scope.

The primary contribution of this study lies in the development of a flexible hybrid modeling framework capable of evaluating diverse infectious disease

interventions. Future research will focus on refining and expanding this framework to better capture the complexities of disease dynamics and vaccination behaviors, ultimately aiming to enhance population-level medical decision-making and public health outcomes.

Conflicts of interest: No conflicts of interest.

Funding: Supported by the National Natural Science Foundation of China (Project Nos. 82473732 to Fang Shao, 82404383 to Mengyi Lu, 82173620 and 82373690 to Yang Zhao, and 82204156 to Dongfang You). Additional funding was provided through the Priority Academic Program Development of Jiangsu Higher Education Institutions (PAPD). The study also received partial support from the Bill & Melinda Gates Foundation (Project No. INV-006371 to Feng Chen).

doi: 10.46234/ccdcw2024.265

[#] Corresponding authors: Fang Shao, shaofang@njmu.edu.cn; Mengyi Lu, mylunjyk@njmu.edu.cn.

[1] Department of Biostatistics, School of Public Health, National Vaccine Innovation Platform, Nanjing Medical University, Nanjing City, Jiangsu Province, China; [2] Pharmaceutical Industry Technology Research Institute of Nanjing Medical University, Taizhou City, Jiangsu Province, China; [3] Nanjing Hanwei Public Health Research Institute Co., Ltd, Nanjing City, Jiangsu Province, China; [4] China International Cooperation Center for Environment and Human Health, Center for Global Health, Nanjing Medical University, Nanjing City, Jiangsu Province, China.

Submitted: April 15, 2024
Accepted: October 18, 2024
Issued: December 13, 2024

REFERENCES

1. Wu XL, Ye ZJ, Xie X, Huang F, Kong DF, Feng TJ, et al. Based on a Markov model, cost-effectiveness analysis of influenza vaccination among people aged 60 years and older in Shenzhen. Chin J Epidemiol 2022;43(7):1140 – 6. https://doi.org/10.3760/cma.j.cn112338-20211221-01005.
2. Yang J, Atkins KE, Feng LZ, Baguelin M, Wu P, Yan H, et al. Cost-effectiveness of introducing national seasonal influenza vaccination for adults aged 60 years and above in mainland China: a modelling analysis. BMC Med 2020;18(1):90. https://doi.org/10.1186/s12916-020-01545-6.
3. National Immunization Advisory Committee (NIAC) Technical Working Group (TWG), Influenza Vaccination TWG. Technical guidelines for seasonal influenza vaccination in China (2023-2024). Chin J Epidemiol 2023;44(10):1507 – 30. https://doi.org/10.3760/cma.j.cn112338-20230908-00139.
4. Wang YJ, Wang P, Zhang SD, Pan H. Uncertainty modeling of a modified SEIR epidemic model for COVID-19. Biology (Basel) 2022;11(8):1157. https://doi.org/10.3390/biology11081157.
5. Bednarski S, Cowen LLE, Ma JL, Philippsen T, van den Driessche P, Wang MT. A contact tracing SIR model for randomly mixed populations. J Biol Dyn 2022;16(1):859 – 79. https://doi.org/10.1080/17513758.2022.2153938.
6. Zhao ZY, Zhou Y, Guan JX, Yan Y, Zhao J, Peng ZH, et al. The relationship between compartment models and their stochastic counterparts: a comparative study with examples of the COVID-19 epidemic modeling. J Biomed Res 2024;38(2):175 – 88. https://doi.org/10.7555/JBR.37.20230137.
7. National Bureau of Statistics of China. China statistical yearbook 2023. Beijing: China Statistics Press. 2023. https://book.kongfz.com/434397/6853349509. (In Chinese).
8. Yang J, Jit M, Zheng YM, Feng LZ, Liu XX, Wu JT, et al. The impact of influenza on the health related quality of life in China: an EQ-5D survey. BMC Infect Dis 2017;17(1):686. https://doi.org/10.1186/s12879-017-2801-2.
9. You XY, Zhang YL, Zeng JF, Wang CJ, Sun HP, Ma QH, et al. Disparity of the Chinese elderly's health-related quality of life between urban and rural areas: a mediation analysis. BMJ Open 2019;9(1):e024080. https://doi.org/10.1136/bmjopen-2018-024080.
10. Yang J, Jit M, Leung KS, Zheng YM, Feng LZ, Wang LP, et al. The economic burden of influenza-associated outpatient visits and hospitalizations in China: a retrospective survey. Infect Dis Poverty 2015;4:44. https://doi.org/10.1186/s40249-015-0077-6.
11. Yue XM, Li YX, Wu JH, Guo JJ. Current development and practice of pharmacoeconomic evaluation guidelines for universal health coverage in China. Value Health Reg Issues 2021;24:1 – 5. https://doi.org/10.1016/j.vhri.2020.07.580.
12. Wang Q, Yue N, Zheng MY, Wang DL, Duan CX, Yu XG, et al. Influenza vaccination coverage of population and the factors influencing influenza vaccination in mainland China: a meta-analysis. Vaccine 2018;36(48):7262 – 9. https://doi.org/10.1016/j.vaccine.2018.10.045.
13. Molinari NAM, Ortega-Sanchez IR, Messonnier ML, Thompson WW, Wortley PM, Weintraub E, et al. The annual impact of seasonal influenza in the US: measuring disease burden and costs. Vaccine 2007;25(27):5086 – 96. https://doi.org/10.1016/j.vaccine.2007.03.046.
14. Jefferson T, Rivetti A, Di Pietrantonj C, Demicheli V. Vaccines for preventing influenza in healthy children. Cochrane Database Syst Rev 2018;2(2):CD004879. https://doi.org/10.1002/14651858.CD004879.pub5.
15. Demicheli V, Jefferson T, Ferroni E, Rivetti A, Di Pietrantonj C. Vaccines for preventing influenza in healthy adults. Cochrane Database Syst Rev 2018;2(2):CD001269. https://doi.org/10.1002/14651858.CD001269.pub6.

SUPPLEMENTARY MATERIAL

Methods

Our proposed hybrid model integrates a continuous-time agent-based model (ABM) with a Markov model for vaccination uptake, incorporating the susceptible-exposed-infected-hospitalized-removed/recovered (SEIHR) framework for epidemic transmission dynamics.

The SEIHR model was implemented to simulate epidemic spread within a randomly mixed population. This model, an extension of the SEIR framework, was adapted from Yanjin Wang, Pei Wang et al. (*1*), who studied COVID-19 transmission in Wuhan following lockdown measures, when population movement was restricted and disease control measures were in place. The population was stratified into five compartments: susceptible (S), exposed (E), infected (I), hospitalized (H), and removed/recovered (R). Given the relatively short time horizon, population dynamics and disease-related mortality were considered negligible; thus, the total population size N remained constant, and a death state was not included. The infected compartment represented outpatient cases, with severe cases transitioning to the hospitalized state and others moving directly to the removed state upon recovery. The SEIHR model dynamics are described by the following system of nonlinear ordinary differential equations.

$$\begin{cases} \frac{dS(t)}{dt} = -\beta\left(1-\frac{I(t)}{N}\right)\frac{I(t)}{N}S(t) \\ \frac{dE(t)}{dt} = \beta\left(1-\frac{I(t)}{N}\right)\frac{I(t)}{N}S(t) - \lambda E(t) \\ \frac{dI(t)}{dt} = \lambda E(t) - \alpha I(t) - \gamma I(t) \\ \frac{dH(t)}{dt} = \alpha I(t) - \mu H(t) \\ \frac{dR(t)}{dt} = \gamma I(t) + \mu H(t) \end{cases}$$

Here, N represents the total population size, $N = S(t) + E(t) + I(t) + H(t) + R(t)$; denotes the progression rate from state S to E; λ represents the rate of progression to I; α indicates the daily rate of progression from infected to hospitalized state; γ represents the recovery rate from I to R; and μ denotes the daily rate of progression from H to R.

A continuous-time agent-based SEIHR model for a randomly mixed population was developed by transforming the compartmental model into an ABM framework. The mathematical equivalence between deterministic compartmental models and their corresponding stochastic ABMs has been established in the literature (*2*–*3*). Individual vaccination status was modeled through a Markov process based on ABM simulation outcomes and vaccination compliance strategies. This innovative integration of a continuous-time ABM with a Markov model enables comprehensive economic evaluation of vaccination compliance strategies for infectious diseases. The schematic representations of the SEIHR model and the hybrid model are illustrated in Figure 1A and 1B, respectively. A detailed description of our proposed hybrid model follows.

The influenza transmission dynamics were simulated through random interactions within the baseline population. An initial population of N agents was generated according to age group proportions. In the first cycle (365 days), agents were randomly selected for vaccination based on age-specific baseline coverage rates. A proportion of agents equal to N times the attack rate was randomly designated as infected (I), with the remaining agents classified as susceptible (S). Each agent was assigned five potential events, with event times determined by adding a waiting time to the current time. These events comprised:

An exposure event for susceptible agents, with waiting time drawn from an exponential distribution parameterized by the age-specific exposure rate β multiplied by the corresponding age-specific exposure vaccination multiplier ($m_{\beta v}$), if applicable (i.e., $\beta m_{\beta v}$);

An infection event for exposed agents, with waiting time drawn from an exponential distribution parameterized by the age-specific rate λ;

A hospitalization event for infected agents, with waiting time drawn from an exponential distribution parameterized by the age-specific infection rate α multiplied by the corresponding age-specific hospitalization

vaccination multiplier ($m_{\alpha v}$), if applicable (i.e., $\alpha m_{\alpha v}$);

A hospitalization progression event for infected agents, with waiting time drawn from an exponential distribution parameterized by the age-specific rate μ;

A recovery event for hospitalized agents, with waiting time drawn from an exponential distribution parameterized by the age-specific rate γ.

The vaccination multipliers were implemented to modify the exposure rate (β) and hospitalization rate (α) for agents across different age groups based on vaccination status. Vaccinated agents' exposure rates were adjusted by the exposure vaccination multiplier ($m_{\beta v}$), resulting in an effective exposure rate of $\beta m_{\beta v}$. Similarly, their hospitalization rates were modified by the hospitalization vaccination multiplier ($m_{\alpha v}$), yielding an effective rate of $\alpha m_{\alpha v}$. Unvaccinated agents retained their baseline rates (β and α, respectively). These multipliers quantified the protective effects of vaccination by reducing the probability of exposure and hospitalization among vaccinated individuals.

The simulation progressed sequentially through event times, with states updated according to the following algorithm.

For exposed/transmission events, a contact was randomly selected assuming uniform population distribution. If the selected contact was in a susceptible state, they transitioned to an exposed state, and an infection event was subsequently scheduled for the exposed agent.

For infection events, the agent transitioned to the infected state, with both recovery and hospitalization events scheduled for the infected individual.

For hospitalization events, the agent transitioned to the hospitalized state, with a recovery event scheduled for their hospitalized status.

For recovery events, the agent was classified as removed, and all remaining scheduled events for that agent were cleared. The removed agent gained immunity and became non-susceptible to infection for the duration of the current cycle.

Events were processed chronologically, with the earliest event executed first, followed by evaluation of subsequent events. This sequence continued until either all events were processed or the simulation reached its designated endpoint of one year (365 days).

Following the ABM simulation cycle, population-wide vaccination for the subsequent cycle was implemented using a Markov model. Each agent's vaccination probability for the next cycle was determined by the vaccination compliance policy, based on both their infection status at the conclusion of the ABM simulation and their vaccination status at the start of the current cycle. The ABM simulation process was then repeated. Each complete cycle consisted of a Markov model-based vaccination process followed by an ABM disease propagation simulation, with multiple cycles executed according to the specified duration. This framework constituted our continuous-time hybrid model combining ABM and Markov approaches for evaluating vaccination compliance strategies in infectious disease contexts.

Hybrid Model Simulation

The analysis of vaccination coverage across five annual cycles (Supplementary Table S1 and Supplementary Figure S1) reveals distinct patterns between the "volunteer" and "adherence" strategies.

SUPPLEMENTARY TABLE S1. Additional parameter settings for PSA.

Parameters	Age groups					
	Age group 1 (≤19 years old)		Age group 2 (20–64)		Age group 3 (≥65)	
	Value	Distribution	Value	Distribution	Value	Distribution
Attack rate	(0.008, 0.012)	Uniform	(0.008, 0.012)	Uniform	(0.008, 0.012)	Uniform
Baseline vaccination coverage	(0.226, 0.276)	Uniform	(0.064, 0.070)	Uniform	(0.238, 0.297)	Uniform
QALY multiplier	(0.95, 1.05)	Uniform	(0.95, 1.05)	Uniform	(0.95, 1.05)	Uniform
Cost per day multiplier	I: (448.51, 0.35) H: (178.55, 4.67)	Gamma	I: (448.51, 0.35, 0) H: (178.55, 4.67, 234.79)	Noncentral Gamma	I: (448.51, 0.35) H: (178.55, 4.67)	Gamma

Note: Uniform (a,b) represents the uniform distribution with minimum a and maximum b. Gamma (a,b) represents the gamma distribution with shape parameter a and scale parameter b. Noncentral gamma (a,b,c) represents the noncentral gamma distribution with shape parameter a, scale parameter b, and noncentrality parameter c.

Abbreviation: PSA=probabilistic sensitivity analysis; QALY=quality-adjusted life year.

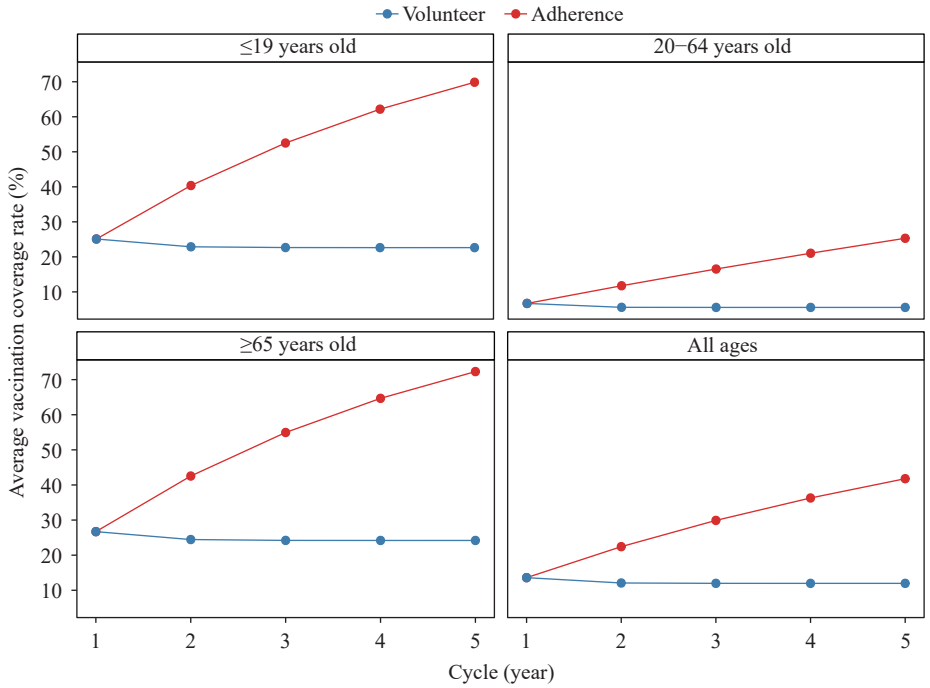

SUPPLEMENTARY FIGURE S1. Average vaccination coverage over five annual cycles of the hybrid model simulation results for the influenza vaccination compliance strategies.

Under the "volunteer" strategy, vaccination decisions are made annually based on individuals' influenza infection experience in the previous year. The general population's average coverage showed a modest decline, starting at 13.6% in Cycle 1 and decreasing to 12.0% by Cycle 5. Coverage among those ≤19 years old decreased from 25.1% to 22.6%, potentially reflecting lower perceived influenza risk in this age group. The 20-64 years age group maintained the lowest coverage, declining from 6.7% to 5.6%. The ≥65 years group sustained the highest coverage, though decreasing from 26.7% to 24.2%.

The "volunteer" strategy demonstrated a characteristic pattern of initial decline followed by stabilization. After the general population's coverage dropped from 13.6% to 12.0% between Cycles 1 and 2, it maintained this level through Cycle 5. Similarly, the ≤19 years group stabilized at 22.9% after an initial decrease from 25.1%, while the 20–64 years group leveled at 5.6% following a decline from 6.7%. The ≥65 years group's coverage stabilized at 24.4% after decreasing from its initial 26.7%.

Under the "adherence" strategy, individuals who have previously received vaccination maintain their vaccination status in subsequent years, while those who have not been vaccinated follow decision-making patterns similar to the "volunteer" strategy, basing their annual vaccination decisions on their previous year's influenza experience. This approach yields substantially higher and progressively increasing coverage rates. The general population's average coverage initiated at 13.6% in Cycle 1 (matching the "volunteer" strategy's baseline) but demonstrated significant growth, reaching 41.8% by Cycle 5. The youngest age group exhibited remarkable improvement from 25.1% to 69.9%, illustrating the cumulative effect of sustained vaccination behavior. The 20–64 years group, despite starting at a lower 6.7%, achieved a substantial increase to 25.3%. The oldest group demonstrated the most pronounced improvement, with coverage expanding from 26.7% in Cycle 1 to 72.3% in Cycle 5.

The marked increase in coverage under the "adherence" strategy can be attributed to its built-in continuity mechanism, which maintains individuals' vaccination status once initiated. This contrasts sharply with the "volunteer" strategy, where despite annual decision opportunities, coverage shows an initial decline followed by stabilization, as vaccination decisions remain solely dependent on the previous year's influenza experience.

Figure 2 presents a comprehensive cost-effectiveness evaluation of both strategies across all cycles through four key analytical visualizations.

The comprehensive analysis of vaccination coverage and cost-effectiveness metrics demonstrates clear advantages of the "adherence" strategy over the "volunteer" approach. The "adherence" strategy's superior effectiveness and

cost-effectiveness, particularly at higher WTP thresholds, stem from its sustained vaccination patterns. The resulting improvements in health outcomes, measured in QALYs, provide robust justification for the strategy's increased implementation costs across multiple WTP thresholds.

Probabilistic Sensitivity Analysis

We conducted probabilistic sensitivity analysis by establishing probability distributions for key parameters including attack rate, baseline vaccination coverage, QALY multiplier, and cost per day multiplier. The complete parameter specifications are detailed in Supplementary Table S2. The comprehensive results are presented in Supplementary Tables S3–S4, Supplementary Figures S2–S3.

The PSA results corroborated our primary hybrid model simulation findings. The incremental cost-effectiveness ratio was 34,432 Chinese Yuan (CNY), marginally higher than the CNY33,847 calculated in the primary analysis (Supplementary Table S3). Vaccination coverage patterns across the five annual cycles closely mirrored those observed in the primary analysis (Supplementary Table S3 and Supplementary Figure S2). In the cost-effectiveness plane (Supplementary Figure S3A), the WTP threshold of CNY85,698 is represented by a dashed line, with points below this line indicating cost-effective outcomes. The analysis revealed that 74.1% of simulated points were cost-effective, with 29.4% demonstrating dominance through both cost savings and health improvements. The cost-effectiveness acceptability curve (Supplementary Figure S3B) and cost-effectiveness acceptability frontier (Supplementary Figure S3C) demonstrated that the "adherence" strategy's probability of cost-effectiveness increases substantially when the WTP exceeds the ICER of CNY34,432, indicating its superiority over the "volunteer" strategy. However, the convergence to complete cost-effectiveness probability was more gradual compared to the

SUPPLEMENTARY TABLE S2. Average vaccination coverage over five annual cycles of the hybrid model simulation results for the influenza vaccination compliance strategies.

Age group (years old)	Cycle (year)	Average vaccination coverage rate (%) (95% *CI*)	
		"Adherence" strategy	"Volunteer" strategy
All ages	1	13.594 (13.592, 13.596)	13.594 (13.592, 13.596)
	2	12.078 (12.076, 12.080)	22.426 (22.423, 22.428)
	3	11.978 (11.976, 11.980)	29.904 (29.901, 29.907)
	4	11.970 (11.968, 11.972)	36.289 (36.286, 36.292)
	5	11.971 (11.969, 11.973)	41.785 (41.782, 41.788)
Age group 1 (≤19)	1	25.100 (25.095, 25.106)	25.100 (25.095, 25.106)
	2	22.874 (22.869, 22.880)	40.370 (40.363, 40.376)
	3	22.661 (22.656, 22.667)	52.512 (52.505, 52.518)
	4	22.635 (22.630, 22.641)	62.174 (62.167, 62.180)
	5	22.639 (22.633, 22.645)	69.866 (69.859, 69.872)
Age group 2 (20–64)	1	6.701 (6.699, 6.703)	6.701 (6.699, 6.703)
	2	5.592 (5.591, 5.594)	11.752 (11.749, 11.754)
	3	5.563 (5.562, 5.565)	16.527 (16.524, 16.530)
	4	5.564 (5.562, 5.565)	21.040 (21.036, 21.043)
	5	5.564 (5.562, 5.566)	25.307 (25.303, 25.310)
Age group 3 (≥65)	1	26.702 (26.695, 26.710)	26.702 (26.695, 26.710)
	2	24.451 (24.444, 24.458)	42.541 (42.533, 42.549)
	3	24.207 (24.200, 24.214)	54.945 (54.937, 54.953)
	4	24.192 (24.185, 24.199)	64.670 (64.662, 64.678)
	5	24.191 (24.184, 24.198)	72.294 (72.287, 72.301)

Note: The outcome values are estimated average vaccination coverage percentages. 95% of *CI*s are obtained by the Clopper and Pearson method (*4*).
Abbreviation: *CI*=confidence interval.

SUPPLEMENTARY TABLE S3. Summary of the hybrid model PSA results for the influenza vaccination compliance strategies.

Outcome	"Adherence" *vs.* "Volunteer" [Estimate (95% *CI*)]
Incremental vaccination number	823.154 (822.438, 823.870)
Decremental infection number	22.506 (22.344, 22.667)
Decremental inpatient number	19.577 (19.436, 19.719)
Decremental outpatient number	2.928 (2.906, 2.951)
Incremental vaccination ratio (%)	133.658 (133.470, 133.846)
Decremental infection ratio (%)	16.252 (16.206, 16.298)
Decremental inpatient ratio (%)	15.833 (15.785, 15.880)
Decremental outpatient ratio (%)	19.746 (19.681, 19.811)
WTP threshold (CNY)	85,698
Incremental QALYs	0.091 (0.066, 0.122)
Incremental costs (CNY)	3,118 (−8,124, 13,409)
Incremental NMB (CNY)	4,642 (−6,878, 16,965)
ICER (CNY per QALY)	34,432

The outcome values are for every 1,000 individuals for 5 years.
Abbreviation: *CI*=confidence interval; CNY=Chinese Yuan; ICER=incremental cost-effectiveness ratio; NMB=net monetary benefit; PSA=probabilistic sensitivity analysis; QALY=quality-adjusted life year; WTP=willingness to pay.

SUPPLEMENTARY TABLE S4. Average vaccination coverage over five annual cycles of the hybrid model PSA results for the influenza vaccination compliance strategies.

Age group (years old)	Cycle (year)	Average vaccination coverage rate (%) (95% *CI*)	
		"Adherence" strategy	"Volunteer" strategy
All ages	1	13.598 (13.596, 13.600)	13.598 (13.596, 13.600)
	2	12.087 (12.085, 12.089)	22.424 (22.421, 22.426)
	3	11.988 (11.986, 11.990)	29.895 (29.892, 29.898)
	4	11.981 (11.979, 11.983)	36.271 (36.268, 36.274)
	5	11.978 (11.976, 11.980)	41.759 (41.756, 41.762)
Age group 1 (≤19 years old)	1	25.131 (25.126, 25.137)	25.131 (25.126, 25.137)
	2	22.917 (22.911, 22.923)	40.395 (40.388, 40.401)
	3	22.705 (22.700, 22.711)	52.522 (52.516, 52.529)
	4	22.683 (22.677, 22.689)	62.165 (62.158, 62.171)
	5	22.674 (22.669, 22.680)	69.839 (69.833, 69.845)
Age group 2 (20–64)	1	6.699 (6.697, 6.701)	6.699 (6.697, 6.701)
	2	5.592 (5.590, 5.594)	11.749 (11.747, 11.752)
	3	5.562 (5.560, 5.564)	16.523 (16.520, 16.526)
	4	5.562 (5.560, 5.564)	21.035 (21.031, 21.038)
	5	5.563 (5.561, 5.565)	25.300 (25.297, 25.304)
Age group 3 (≥65)	1	26.690 (26.683, 26.697)	26.690 (26.683, 26.697)
	2	24.455 (24.448, 24.462)	42.501 (42.493, 42.508)
	3	24.220 (24.213, 24.227)	54.884 (54.876, 54.892)
	4	24.202 (24.195, 24.209)	64.587 (64.579, 64.595)
	5	24.197 (24.190, 24.204)	72.190 (72.183, 72.197)

Note: The outcome values are estimated average vaccination coverage percentages. 95% of *CI*s are obtained by the Clopper and Pearson method (*4*).
Abbreviation: *CI*=confidence interval; PSA=probabilistic sensitivity analysis.

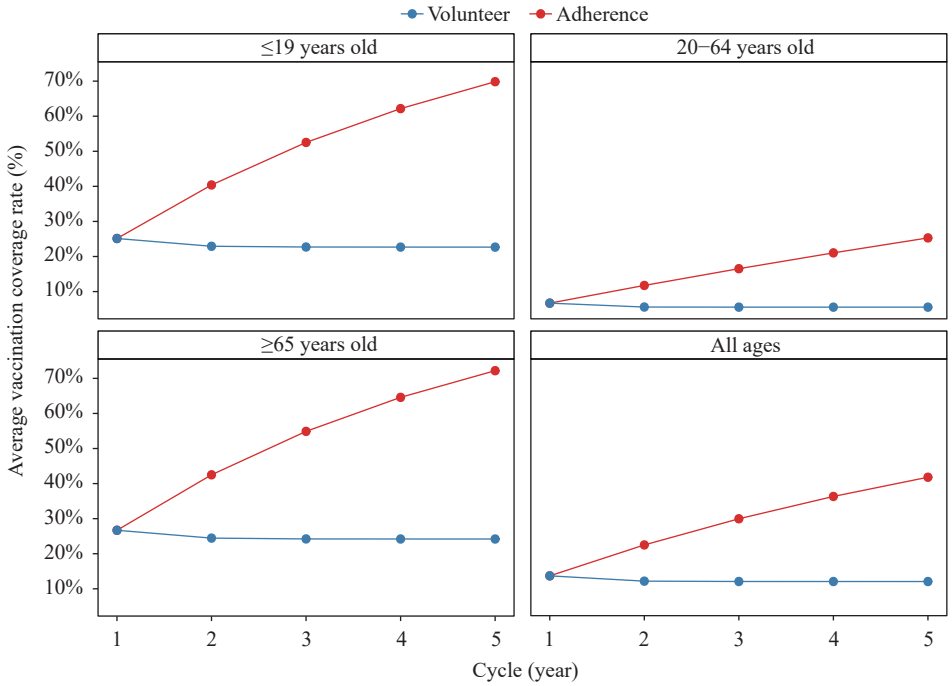

SUPPLEMENTARY FIGURE S2. Average vaccination coverage over five annual cycles of the hybrid model PSA results for the influenza vaccination compliance strategies.
Abbreviation: PSA=probabilistic sensitivity analysis.

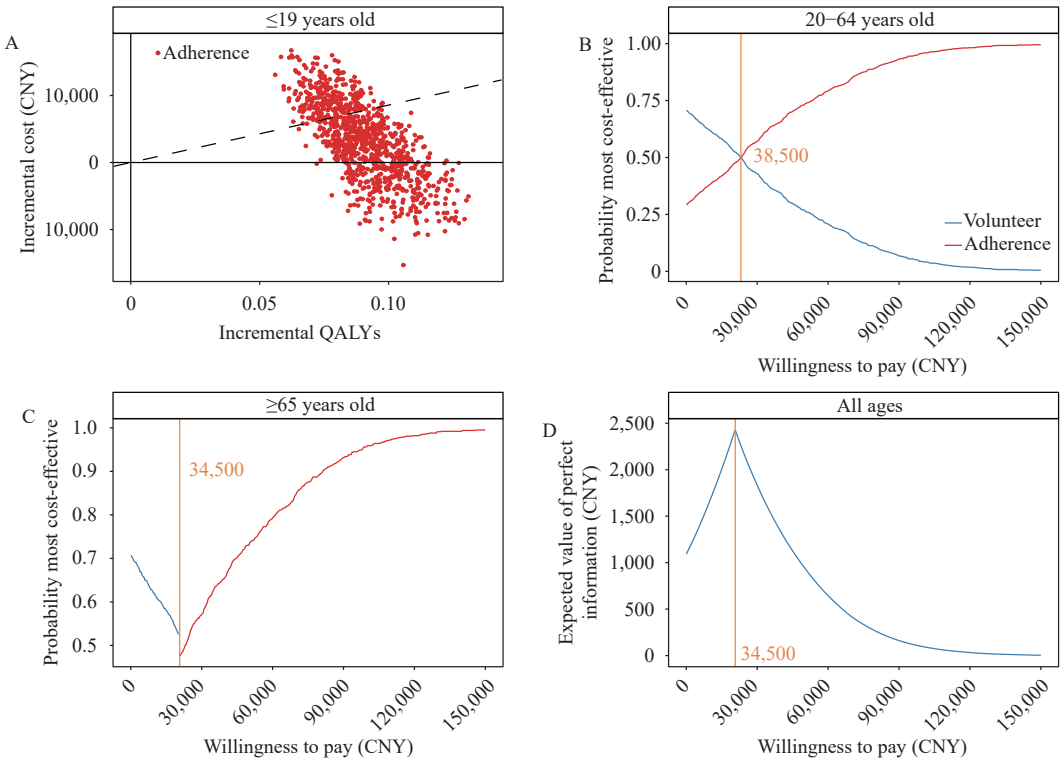

SUPPLEMENTARY FIGURE S3. Cost-effectiveness analysis results for the PSA of the hybrid model simulations. (A) The cost-effectiveness plane. The dashed line represents the WTP threshold (85,698 CNY). (B) The cost-effectiveness acceptability curves. (C) The cost-effectiveness acceptability frontier. (D) The expected value of perfect information.
Note: The costs and QALYs are reported for every 1,000 individuals for 5 years. The population size is *N*=1,000,000 with 1,000 simulation replicates.
Abbreviation: CNY=Chinese Yuan; PSA=probabilistic sensitivity analysis; QALY=quality-adjusted life year; WTP=willingness to pay.

primary analysis. Similarly, the expected value of perfect information peaked near the ICER threshold (Supplementary Figure S3D), quantifying the potential value of uncertainty reduction through additional research. While following the same pattern as the primary analysis, the EVPI's convergence to zero occurred more gradually.

R Code

The simulation's demonstrative R code is available online as a separate file (demo.R) at https://gitee.com/jimmy838/continuous-time-agent-based-markov-hybrid-model/blob/master/demo.R.

REFERENCES

1. Wang YJ, Wang P, Zhang SD, Pan H. Uncertainty modeling of a modified SEIR epidemic model for COVID-19. Biology (Basel) 2022;11(8):1157. https://doi.org/10.3390/biology11081157.
2. Bednarski S, Cowen LLE, Ma JL, Philippsen T, van den Driessche P, Wang MT. A contact tracing SIR model for randomly mixed populations. J Biol Dyn 2022;16(1):859 – 79. https://doi.org/10.1080/17513758.2022.2153938.
3. Zhao ZY, Zhou Y, Guan JX, Yan Y, Zhao J, Peng ZH, et al. The relationship between compartment models and their stochastic counterparts: a comparative study with examples of the COVID-19 epidemic modeling. J Biomed Res 2024;38(2):175 – 88. https://doi.org/10.7555/JBR.37.20230137.
4. Clopper CJ, Pearson ES. The use of confidence or fiducial limits illustrated in the case of the binomial. Biometrika 1934;26(4):404 – 13. https://doi.org/10.1093/biomet/26.4.404.